

**SAMP1 mice as a new animal model for photoaging
of the skin associated with spontaneous higher
oxidative stress status**

MASAAKI SAKURA

Contents

| | |
|--|----|
| Abbreviations | 3 |
| General Introduction | 4 |
| CHAPTER 1. Spontaneous occurrence of photoaging-like phenotypes in the dorsal skin of old SAMP1 mice, an oxidative stress model | |
| Abstract | 9 |
| Introduction | 10 |
| Materials and Methods | 13 |
| Results | 18 |
| Discussion | 34 |
| CHAPTER 2. Differences in the histopathology and cytokine expression pattern between chronological aging and photoaging of hairless mice skin | |
| Abstract | 40 |
| Introduction | 42 |
| Materials and Methods | 44 |
| Results | 48 |
| Discussion | 67 |

| | |
|------------------------------|----|
| Conclusion | 70 |
| Acknowledgments | 72 |
| References | 73 |

Abbreviations

ANOVA, analysis of variance

DEJ, dermal-epidermal junction

GAG, glycosaminoglycan

H&E, hematoxylin-eosin

IFN- γ , interferon-gamma

IL-1 β , interleukin-1 beta

IL-6, interleukin-6

iNOS, inducible nitric oxide synthase

MMP, matrix metalloproteinase

PBS, phosphate-buffered saline

ROS, reactive oxygen species

SAMP, senescence-accelerated mouse-prone

SAMR, senescence-accelerated mouse-resistant

TBARS, thiobarbituric acid reactive substances

TGF- β 1, transforming growth factor-beta 1

TNF- α , tumor necrosis factor-alpha

UV, ultraviolet

General Introduction

A major function of skin is to protect organisms from physical and environmental assaults such as solar radiation, infection, or dehydration. These protective functions can decline with age [1]. Aging of the skin is a process in which both intrinsic and extrinsic determinants lead to a progressive loss of structural integrity and physiological function [2]. The intrinsic aging process is characterized by slow and irreversible tissue degeneration, and affects the skin as well as the whole body. The extrinsic aging process, i.e. “photoaging”, is provoked by chronic exposure to sunlight, and especially ultraviolet (UV) light [1,3]. In short, photoaging refers to the effects of long-term UV exposure [1]. Since people are living longer, and spend more spare time outdoors, this leads to excessive exposure to UV radiation from natural sunlight, resulting in an ever increasing demand to protect human skin against the detrimental effects of UV exposure [4]. Photoaged skin is clinically important not only because it causes considerable cosmetic and psychosocial distress in older people, but also because benign, premalignant, and malignant neoplastic growths flourish in photoaged skin [5,6].

UV radiation consists of UVA (320 to 400 nm), UVB (280 to 320 nm) and UVC (200 to 280 nm). More than 90% of UV radiation that reaches the earth is

UVA which penetrates deep into the epidermis and dermis of the skin. Compared to UVB, UVA is more effective in the production of an immediate tanning effect [7]. Although UVB is a minor component, it is the most active constituent of solar light. UVB is 1000 times more capable of causing sunburns and more genotoxic than UVA [7]. The third type of UV radiation, UVC, also called shortwave or ionizing radiation, is absorbed by gas in the atmosphere, and thus does not reach the earth's surface and therefore does not normally contribute to photodamage [8]. As for the pathogenesis of photoaging, reactive oxygen species (ROS) generated by UV radiation are thought to play an integral role.

UV-induced ROS can exert a multitude of effects such as lipid peroxidation, the activation of transcription factors and the generation of DNA strand breaks [1]. Moreover, UV radiation stimulates and activates various cells to produce and release pro-inflammatory cytokines and matrix metalloproteinases (MMPs) that may play important roles in the photoaging process [9].

The most conspicuous stigmata of skin aging appear on sun-exposed areas in the elderly, especially on the face, and results in photoaging. Photoaged skin is histologically characterized by elastosis [10], which generally begins at the junction of the papillary and reticular dermis. Other histological changes characterizing photoaged skin include a large increase in the deposition of glycosaminoglycan (GAG) [11,12], fragmented elastic fibers [13], and the

formation of the Grenz zone [3], which is a narrow band in the uppermost portion of the dermis composed primarily of GAGs and newly formed collagen [14].

The long latency period and slow evolution of photoaging make human studies difficult [3]. Therefore, the development of a reliable animal model is necessary to systematically study the pathogenesis of photoaged skin. At present, UV-irradiated skh-hairless mice are widely used as an animal model for skin photoaging [15]. In this model, UV irradiation generally starts at 6 to 8 weeks of age, and is continued for 10 to 22 weeks to produce photoaging-like skin lesions [16,17]. This model mimics the extrinsic aspects of the pathogenesis of photoaging, and recapitulates many features of human photoaging. However, human photoaging is considered to be the superposition of solar damage on the normal aging process [2], and it is difficult to study the contribution of the intrinsic aging process in the pathogenesis of photoaging using this model. It is important to elucidate how the intrinsic aging process contributes to the pathogenesis of photoaging *in vivo*, since intrinsic factor(s) seems to be essential for the manifestation of skin photoaging phenotypes in humans.

In the present study, I describe senescence-accelerated mouse-prone 1 (SAMP1) strain of mice with higher oxidative status, as a new animal model for human skin photoaging due to exaggerated intrinsic factors. This mouse may be a useful model to study the contribution of intrinsic aging processes in the

pathogenesis of photoaging. Furthermore, I compared the histological changes and cytokine expression patterns between UV-irradiated hairless mice, a standard photoaging model, and non-irradiated, chronologically aged hairless mice to clarify factor(s) that differentiate photoaging from chronological aging phenotypes in the skin.

Finally, an imbalance between pro-inflammatory and anti-inflammatory conditions caused by UV and/or ROS is proposed as a possible pathogenetic factor of the skin photoaging.

CHAPTER 1

Spontaneous occurrence of photoaging-like phenotypes in the dorsal skin of old SAMP1 mice, an oxidative stress model

Abstract

I showed that skin from old senescence-accelerated mouse-prone 1 (SAMP1) mice, a model for accelerated senescence and higher oxidative status, exhibited histological and gene expression changes similar to those in human photoaged skin without UV irradiation. Histopathological analysis revealed an age-associated increase in the elastic fiber and glycosaminoglycan content of the dermis of 48- to 70-week-old SAMP1 mice. I observed an upregulation of several pro-inflammatory cytokines and matrix metalloproteinases-7 and -12 with advancing age in SAMP1 skin. These changes occurred concomitantly with an increase in lipid peroxide levels in the skin. These age-associated changes were not observed in skin from control (long-lived) senescence-accelerated mouse-resistant 1 (SAMR1) mice. I propose that SAMP1 mice are a spontaneous animal model for human photoaging caused by an exaggerated intrinsic mechanism, which is useful to explore the link between oxidative stress and photoaging, and to evaluate the efficacy of antioxidants.

Introduction

As mentioned in the General Introduction, chronic exposure to sunlight is required to develop characteristic stigmata observed in aging skin. Human skin photoaging can be considered to be a superposition of solar damage on the normal aging process [2]. The long latency period and slow evolution of photoaging makes human studies difficult [3]. Therefore, the development of a reliable animal model is necessary to systematically study the pathogenesis of photoaged skin. UV-irradiated skh-hairless mice are widely used as a photoaging model [15]. This model recapitulates many features of human photoaging. However, the aforementioned animal model only mimics the extrinsic aspects of the pathogenesis of photoaging, and the contribution of the intrinsic aging process is difficult to study using this model. As described in the General Introduction, reactive oxygen species (ROS) generated by UV are suspected to be important factors for the pathogenesis of photoaging. ROS are also important factors for senescence and/or age-associated degenerative changes in various tissues [18,19].

The senescence-accelerated mouse (SAM), a group of related inbred strains, was developed as a model of senescence acceleration and geriatric disorders observed in humans [20-23]. These mice consist of a series of SAMP (accelerated senescence-prone, short-lived) and SAMR (accelerated

senescence-resistant, long-lived) strains. SAMP mice show an accelerated senescence process, shorter lifespan and an earlier onset and more rapid progression of age-associated pathological phenotypes when compared to SAMR mice [23,24]. Spontaneous higher oxidative stress status due to mitochondrial dysfunction is thought to be a contributing factor to senescence acceleration and age-associated pathologies in SAMP mice (reviewed in 18,19). Hosokawa *et al.*, revealed that murine dermal fibroblast-like (MDF) cells from dorsal dermis of neonatal SAMP11 mice showed earlier occurrence of senescence/crisis than those from SAMR1 mice [25]. MDF cells from SAMP11 mice showed higher lipid peroxide (LPO) contents than those from SAMR1 mice [26]. Furthermore, supplementation of media with aminoguanidine, an inhibitor of diamine oxidase and nitric oxide synthase, delayed the senescence/crisis and decreased the LPO content in MDF cells from SAMP11 mice to levels found in those from SAMR1 mice [26]. These data suggest that higher oxidative stress in SAMP11 cells may contribute to accelerated senescence *in vitro*. An increase in the production of ROS from MDF cells from SAMP11 mice was also confirmed by live cell imaging, and the main source of ROS production was mitochondria [23]. Mitochondrial function and ultrastructures were also impaired in MDF cells from SAMP11 mice when compared with those from SAMR1 mice [23].

Several studies have addressed aging changes in the skin of SAMP mice.

Changes in the levels of thiobarbituric acid reactive substances (TBARS) occur at middle age, and histological changes at a later age in SAMP1 skin [27]. Okada *et al.*, reported that the deposition of elastic fibers was observed in 12- to 14-month-old SAMP1 skin [28]. After these reports, however, there has been no systematic study to investigate aging changes of SAMP1 skin.

On the basis of these previous studies, I hypothesized that the age-associated skin changes of SAMP1 mice may be similar to photoaged skin. The present study was undertaken to characterize the morphological and biochemical aspects of age-associated changes in the skin from SAMP1 mice, and to test the validity of SAMP1 mice as an animal model for human skin photoaging.

Materials and Methods

Animals

SAMP1 and SAMR1 strains of mice were bred under conventional conditions, housed at $23 \pm 2^\circ\text{C}$, and allowed free access to food (CE2, Nihon CLEA, Tokyo, Japan) and tap water. The light-dark cycle was set at 12 hours (lights were on at 07:00). In SAMP1 mice, the mean life span for the last one tenth of a group of survivors for males was 535 days, and the median survival time for males was 361 days. In SAMR1 mice, which have a normal life span, the mean life span for the last one tenth of a group of survivors for males was 783 days, and the median survival time for males was 634 days [29]. Male SAMP1 mice at 12, 24, 36, 48, 56 and 70 weeks of age and SAMR1 mice at 12 and 70 weeks of age were used. I checked all mice pathologically after sampling the skin specimens, and excluded those samples from mice with inflammation-associated phenotypes (pneumonia and colitis) and/or tumors from the subsequent analyses.

I took special care to minimize the number of animals used and their suffering. All animals were handled in accordance with the Guide for the Care and Use of Laboratory Animal of the Institute for Developmental Research, Aichi Human Service Center.

Histology

Each mouse was sacrificed by cervical dislocation, and the dorsal skin was rapidly removed, immersed in 10% neutral buffered formalin (pH 7.4) for 7 days, and embedded in paraffin. Twenty-micron-thick sections were cut with a sliding microtome, and hematoxylin and eosin (H&E), toluidine blue, resorcin-fuchsin and alcian blue staining procedures were performed according to standard protocols.

The density of mast cells was evaluated using sections stained with toluidine blue. Photomicrographs of continuous, non-overlapping visual fields ($585 \times 424 \mu\text{m}$) were obtained to cover the entire dermis of the specimen using a digital microscope (VHX-200, Keyence Corporation, Osaka, Japan). The mast cells were counted, and the density was calculated by dividing the mast cell number by the evaluated area.

RNA extraction and real-time quantitative PCR

The dorsal skin was dissected from each mouse and washed in ice-cold phosphate-buffered saline (PBS). The total RNA was isolated using an ISOGEN kit (NIPPON GENE CO., LTD., Tokyo, Japan) according to the manufacturer's instructions. The RNA yields and purities were determined by spectrophotometric absorption analyses at 260/280 nm. cDNA was synthesized

from the total RNA using a SuperScriptTM III First-Strand Synthesis System for RT-PCR (Invitrogen, Carlsbad, CA, USA) according to the manufacturer's instructions.

Gene expression was analyzed by a real time RT-PCR system (ABI Stepone-Plus, Applied Biosystems, Foster City, CA, USA) with each cDNA sample, specific Taqman primers/probes and a Taqman Universal PCR Master Mix (Applied Biosystems). The following probes were used (identified by Applied Biosystems assay identification number): IL-1 beta (IL-1 β), Mm00434228_m1; TNF-alpha (TNF- α), Mm00443258_m1; IL-6, Mm00446190_m1; IFN-gamma (IFN- γ), Mm00801778_m1; TGF-beta1 (TGF- β 1), Mm00441724_m1; iNOS, Mm00440485_m1; IL-4, Mm00445260_m1; MMP7, Mm001168420_m1; MMP-12, Mm00500554_m1 and 18S rRNA, Hs99999901_s1. 18S rRNA was used as an internal control. The expression of these mRNA species was analyzed using the same sets of total RNA samples. The reaction mixtures were subjected to the following amplification scheme: 1 cycle at 50°C for 2 min (AmpErase uracil-N-glycosylase deactivation) and 1 cycle at 95°C for 10 min (AmpliTaq Gold activation), followed by 40 cycles at 95°C for 15 s (denaturation) and 60°C for 1 min (annealing and extension).

Measurement of skin thiobarbituric acid reactive substances (TBARS)

The TBARS levels in the skin were measured as a marker of lipid peroxidation [30] using the NWLSS™ Malondialdehyde Assay (Northwest Life Science Specialties, Vancouver, WA, USA). The dorsal skin was removed, frozen in liquid nitrogen and then homogenized with a mortar. The homogenate was mixed with the assay buffer from the kit, mixed vigorously and centrifuged at $10,000 \times g$ for 5 min. The supernatant or standards (250 μ l) were added to test tubes containing 10 μ l of butylated hydroxytoluene. After the addition of 250 μ l of 1 M phosphoric acid and 250 μ l of thiobarbituric acid solution, the tubes were mixed vigorously and incubated for 60 min at 60°C. The mixture was then centrifuged at $10,000 \times g$ for 3 min, and the absorbance spectra were recorded between 400 nm and 700 nm using a spectrophotometer (Ultrospec 2000, Pharmacia Biotech, Cambridge, UK), and the TBARS levels were determined according to the manufacturer's recommendations. The protein concentration in the sample was determined by the Bradford assay using bovine serum albumin as the standard.

Statistical Analyses

The data were expressed as means \pm S.D. A one-way analysis of variance (ANOVA) followed by Tukey's procedure were performed to determine the

differences in the expression of mRNA and skin TBARS levels among different age groups of SAMP1 mice. A two-way ANOVA, followed by a simple main effects analysis was performed to examine the difference in the expression of mRNA and the skin TBARS levels among 12- and 70-week-old SAMP1 and SAMR1 mice. The number of mast cells between 12- and 70-week-old SAMP1 mice was compared using Student's t-test. Differences were considered to be statistically significant when $p < 0.05$.

Results

Histological analyses of age-associated changes in SAMP1 versus SAMR1 skin

H&E staining revealed an increase in the area of flattened dermal-epidermal junctions (DEJ), in the number of immature fibroblasts beneath the epidermis, and in the epidermal thickness at 56 and 70 weeks of age in SAMP1 mice (Fig. 1e, f). Irregularity in the direction of hair shaft growth (Fig. 1e, f) and the formation of Grenz zones (Fig. 1e, f, asterisks) were observed in 56- and 70-week-old SAMP1 mice. In contrast, 70-week-old SAMR1 mice did not exhibit any significant age-related changes in the skin when compared to 12-week-old SAMR1 mice (Fig. 1g, h).

Toluidine blue staining revealed that the number of infiltrating mast cells was increased in the dermis of SAMP1 mice at 70 weeks of age. The number of mast cells at 70 weeks of age was 3.1-fold greater than that at 12 weeks of age (267.3 ± 172.4 vs. $86.0 \pm 7.84/\text{mm}^2$, $p = 0.047$). In contrast, 70-week-old SAMR1 mice did not show this increase in dermal mast cells (data not shown).

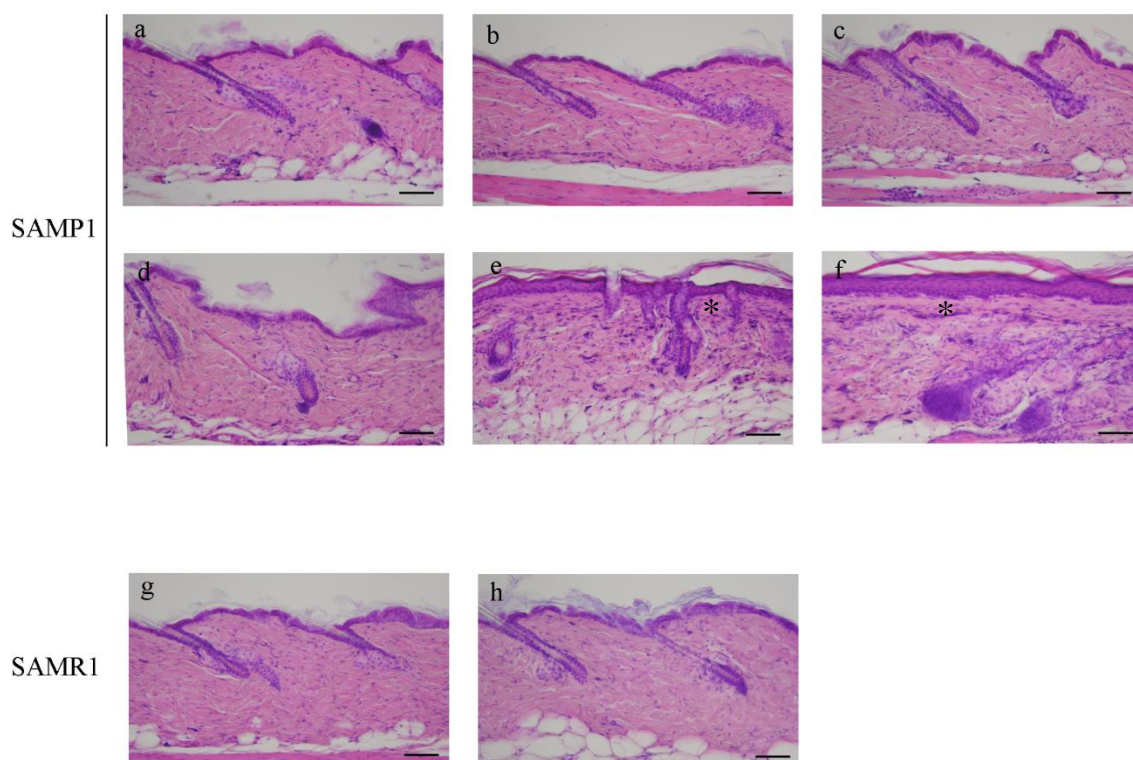


Fig. 1. Histological changes in SAMP1 and SAMR1 mouse dorsal skin revealed by hematoxylin and eosin (H&E) staining. Representative photomicrographs of the dorsal skin from 12- (a), 24- (b), 36- (c), 48- (d), 56- (e) and 70-week-old (f) SAMP1 mice and 12- (g) and 70-week-old (h) SAMR1 mice. Formalin-fixed skin sections were stained with H&E. Asterisk in e and f indicates Grenz zone. See the text for the detailed description. Scale bars: 100 μ m.

Using resorcin-fuchsin staining, numerous fine and highly branched elastic fibers were deposited in the dermis of SAMP1 mice, which first appeared at 48 weeks of age (Fig. 2d), and increased until 70 weeks of age (Fig. 2e, f) to develop overt elastosis (Fig. 2f, open arrowhead). In SAMR1 mice, resorcin-fuchsin staining did not show any age-related changes in the dermal elastic fibers (Fig. 2g, h).

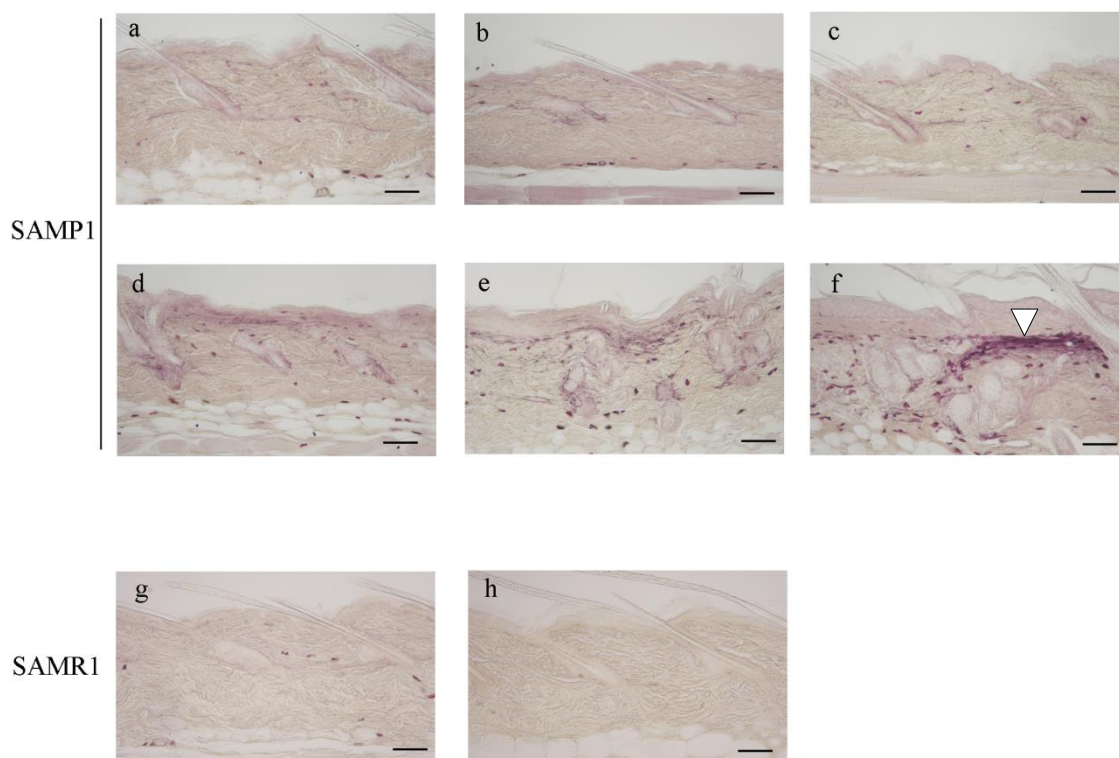


Fig. 2. Histological changes in SAMP1 and SAMR1 mouse dorsal skin revealed by resorcin-fuchsin staining.

Representative photomicrographs of the dorsal skin from 12- (a), 24- (b), 36- (c), 48- (d), 56- (e) and 70-week-old (f) SAMP1 mice and 12- (g) and 70-week-old (h) SAMR1 mice.

Formalin-fixed skin sections were stained with resorcin-fuchsin. The open arrowhead in f indicates overt elastosis in the dermis. See the text for the detailed description. Scale bars: 100 μm .

In alcian blue-stained sections, a prominent accumulation of alcian blue-positive GAGs was observed just beneath the epidermis at 48 weeks of age in SAMP1 mice (Fig. 3d, closed arrowheads), and the GAG-positive area spread toward the deep layer of the dermis with advancing age (Fig. 3e, f). Again, 70-week-old SAMR1 mice did not show any changes in the GAG volume in their dermis when compared to 12-week-old SAMR1 mice (Fig. 3g, h).

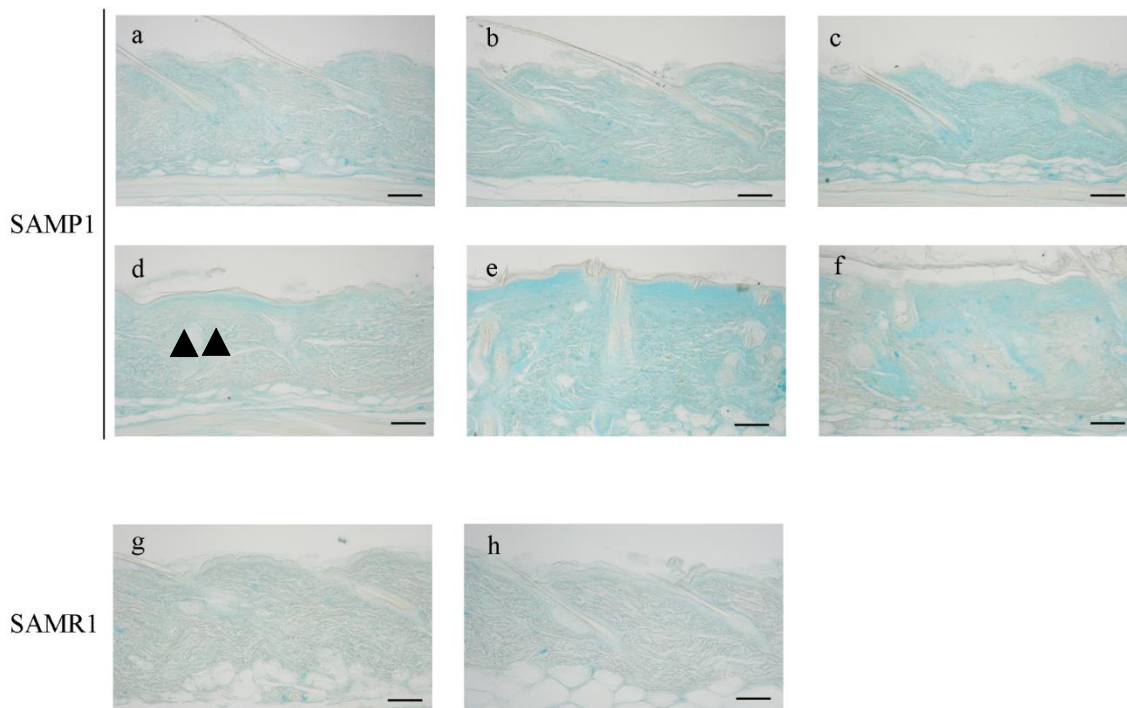


Fig. 3. Histological changes in SAMP1 and SAMR1 mouse dorsal skin revealed by alcian blue staining.

Representative photomicrographs of the dorsal skin from 12- (a), 24- (b), 36- (c), 48- (d), 56- (e) and 70-week-old (f) SAMP1 mice and 12- (g) and 70-week-old (h) SAMR1 mice. Formalin-fixed skin sections were stained with alcian blue. The closed arrowheads in d indicate increased glycosaminoglycans. See the text for the detailed description. Scale bars: 100 μ m.

Gene expression analyses of SAMP1 and SAMR1 skin by real-time PCR

The expression of IL-1 β mRNA tended to change with age in SAMP1 mice ($F(5,28) = 2.482$, $p = 0.0556$). The expression of IL-1 β mRNA peaked at 56 weeks of age, but then decreased at 70 weeks of age. A two-way ANOVA showed a significant interaction between the effects of strain and age on the expression of IL-1 β ($F(1,14) = 14.475$, $p = 0.0019$). Simple main effects analysis revealed that 70-week-old SAMP1 mice showed greater expression than that in SAMR1 mice at the same age, whereas there were no differences between 12-week-old SAMP1 and SAMR1 mice (Fig. 4a).

In the expression of TNF- α mRNA, a one-way ANOVA showed a significant effect for age in SAMP1 mice ($F(5,32) = 8.703$, $p < 0.0001$). The TNF- α mRNA levels of 70-week-old SAMP1 mice were 12.9-fold greater than that of 12-week-old SAMP1 mice. A two-way ANOVA showed a significant interaction between the effects of strain and age on the expression of TNF- α ($F(1,17) = 4.701$, $p = 0.0446$). Simple main effects analysis revealed that 70-week-old SAMP1 mice showed greater expression than that in SAMR1 mice at the same age, whereas there were no differences between 12-week-old SAMP1 and SAMR1 mice (Fig. 4b).

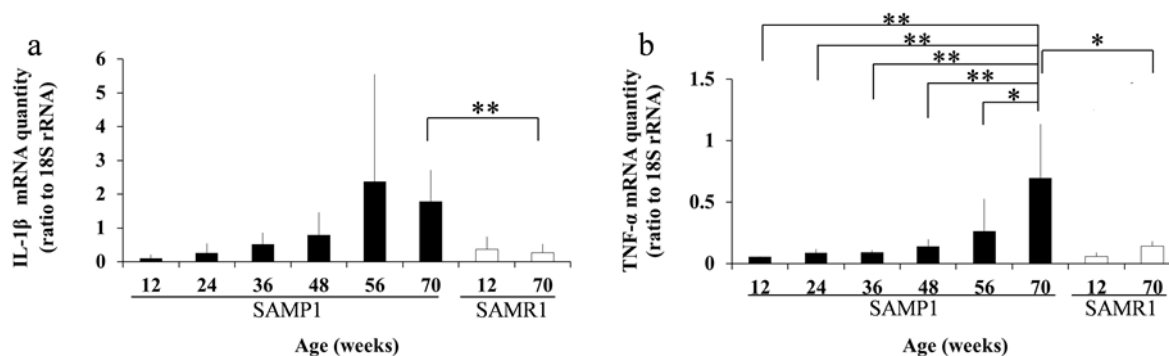


Fig. 4. Expression changes in IL-1 β and TNF- α mRNA in the skin from SAMP1 and SAMR1 mice.

The expression of IL-1 β (a) and TNF- α (b) mRNAs in the skin from SAMP1 and SAMR1 mice were analyzed by real-time PCR. The relative levels of mRNA were obtained by dividing the quantity of each mRNA by that of 18S rRNA as the internal standard. The closed bars represent SAMP1 mice, and the open bars represent SAMR1 mice. All data are presented as means \pm S.D. The number of mice used in this experiment ranged from 4 to 11 for each experimental group. (*) $p < 0.05$, (**) $p < 0.01$.

In the expression of IL-6 mRNA, a one-way ANOVA showed a significant effect for age in SAMP1 mice ($F(5,31) = 3.317$, $p = 0.0163$). The expression of IL-6 mRNA increased dramatically at 56 weeks of age, and then decreased at 70 weeks of age. The expression level of IL-6 mRNA at 56 weeks of age was 6.4-fold higher than that at 12 weeks of age. In a two-way ANOVA, there were no significant interaction between strain and age on the expression of IL-6 ($F(1,15) = 2.776$, $p = 0.116$) (Fig. 5a).

In the expression of IFN- γ mRNA, a one-way ANOVA showed a significant effect for age in SAMP1 mice ($F(5,30) = 5.605$, $p = 0.0009$). The expression of IFN- γ mRNA increased dramatically at 48 weeks of age, and remained high until 70 weeks of age. The mRNA level at 70 weeks of age was 60.7-fold higher than that at 12 weeks of age. A two-way ANOVA showed a significant interaction between the effects of strain and age on the expression of IFN- γ ($F(1,15) = 4.680$, $p = 0.0471$). Simple main effects analysis revealed that 70-week-old SAMP1 mice showed greater expression than that in SAMR1 mice at the same age, whereas there were no differences between 12-week-old SAMP1 and SAMR1 mice (Fig. 5b).

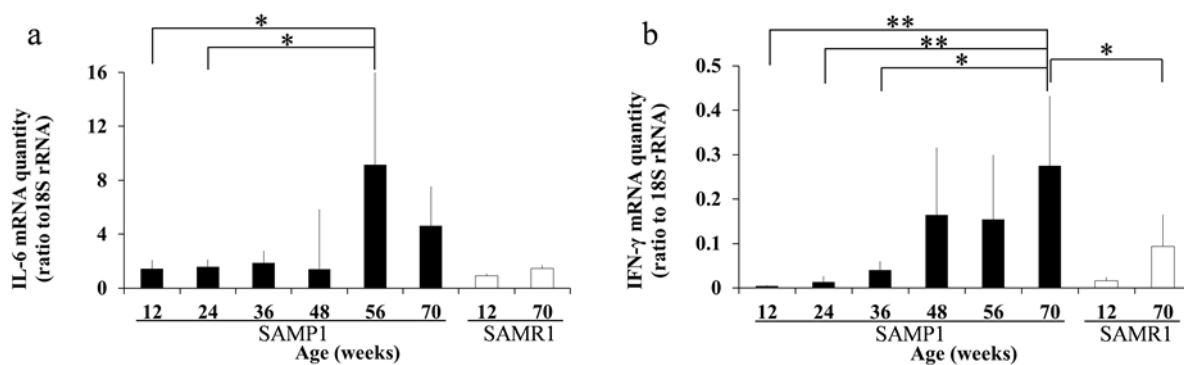


Fig. 5. Expression changes in IL-6 and IFN- γ mRNA in the skin from SAMP1 and SAMR1 mice.

The expression of IL-6 (a) and IFN- γ (b) mRNAs in the skin from SAMP1 and SAMR1 mice were analyzed by real-time PCR. The relative levels of mRNA were obtained by dividing the quantity of each mRNA by that of 18S rRNA as the internal standard. The closed bars represent SAMP1 mice, and the open bars represent SAMR1 mice. All data are presented as means \pm S.D. The number of mice used in this experiment ranged from 4 to 11 for each experimental group. (*) $p < 0.05$, (**) $p < 0.01$.

In the expression of TGF- β 1, a one-way ANOVA showed a significant effect for age in SAMP1 mice ($F(5,36) = 2.737$, $p = 0.0339$). The expression level of TGF- β 1 mRNA at 70 weeks of age was 2.8-fold higher than that at 12 weeks of age. In a two-way ANOVA, there were no significant interaction between strain and age on the expression of TGF- β 1 ($F(1,19) = 0.478$, $p = 0.498$) (Fig. 6a).

In the expression of iNOS mRNA, a one-way ANOVA showed a significant effect for age in SAMP1 mice ($F(5,37) = 5.931$, $p = 0.0004$). The expression of iNOS mRNA increased gradually with age, and the mRNA level at 70 weeks of age was 4.1-fold higher than that at 12 weeks of age. A two-way ANOVA showed a trend for positive interaction on the expression of iNOS ($F(1,23) = 3.750$, $p = 0.0652$) mRNA. The iNOS expression of 70-week-old SAMP1 mice showed a greater expression of these mRNA than SAMR1 mice at the same age (Fig. 6b).

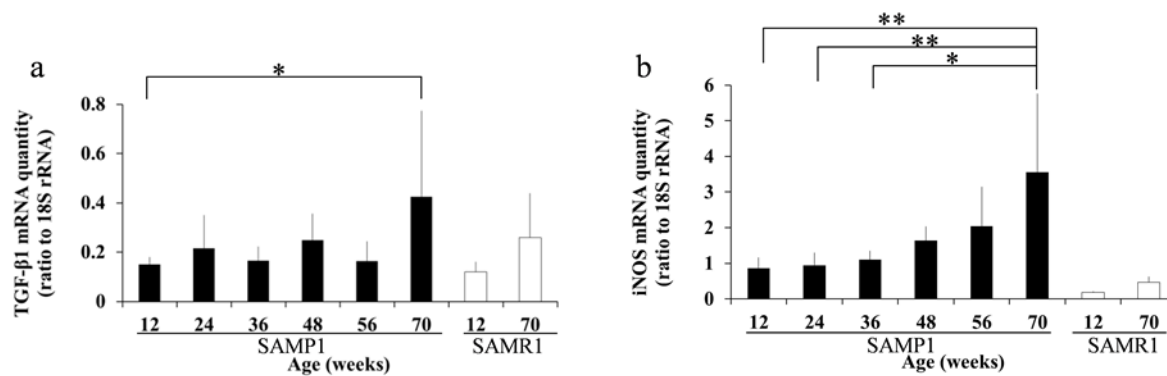


Fig. 6. Expression changes in TGF- β and iNOS mRNA in the skin from SAMP1 and SAMR1 mice.

The expression of TGF- β 1 (a) and iNOS (b) mRNAs in the skin from SAMP1 and SAMR1 mice were analyzed by real-time PCR. The relative levels of mRNA were obtained by dividing the quantity of each mRNA by that of 18S rRNA as the internal standard. The closed bars represent SAMP1 mice, and the open bars represent SAMR1 mice. All data are presented as means \pm S.D. The number of mice used in this experiment ranged from 4 to 11 for each experimental group. (*) $p < 0.05$, (**) $p < 0.01$.

In the expression of MMP-7 mRNA, a one-way ANOVA showed a significant effect for age in SAMP1 mice ($F(5,47) = 5.285$, $p = 0.0007$). The expression of MMP-7 mRNA was very low until 48 weeks of age, and then increased at older ages. The mRNA level at 70 weeks of age was 16.2-fold higher than that at 12 weeks of age. A two-way ANOVA showed a significant interaction between the effects of strain and age on the expression of MMP-7 ($F(1,22) = 4.963$, $p = 0.0364$) mRNA. Simple main effects analysis revealed that 70-week-old SAMP1 mice showed greater expression of these mRNA than SAMR1 mice at the same age, whereas there were no differences between 12-week-old SAMP1 and SAMR1 mice (Fig. 7a).

In the expression of MMP-12 mRNA, a one-way ANOVA showed a significant effect for age in SAMP1 mice ($F(5,27) = 8.584$, $p < 0.0001$). The expression of MMP-12 mRNA increased dramatically at 48 weeks of age, and peaked at 70 weeks of age. The expression level at 70 weeks of age was 4.7-fold higher than that at 12 weeks of age. In a two-way ANOVA, there were no significant interaction between strain and age on the expression of MMP-12 ($F(1,17) = 0.036$, $p = 0.852$) mRNA (Fig. 7b).

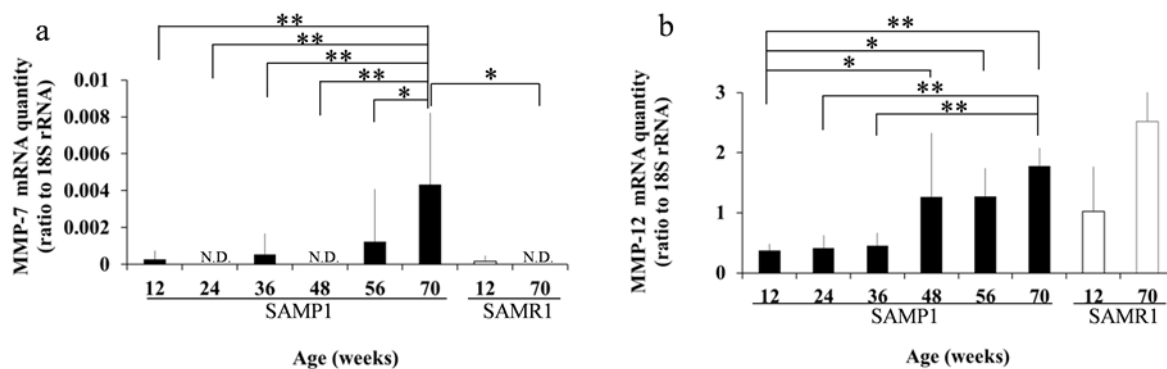


Fig. 7. Expression changes in MMP-7 and MMP-12 mRNA in the skin from SAMP1 and SAMR1 mice.

The expression of MMP-7 (a) and MMP-12 (b) mRNAs in the skin from SAMP1 and SAMR1 mice were analyzed by real-time PCR. The relative levels of mRNA were obtained by dividing the quantity of each mRNA by that of 18S rRNA as the internal standard. The closed bars represent SAMP1 mice, and the open bars represent SAMR1 mice. All data are presented as means \pm S.D. The number of mice used in this experiment ranged from 4 to 11 for each experimental group. (*) $p < 0.05$, (**) $p < 0.01$. N.D.: not detected.

Age-associated changes in the TBARS content in SAMP1 and SAMR1 skin

The extent of lipid peroxidation in the skin was assessed by measuring the TBARS level. A one-way ANOVA showed a significant effect for age in SAMP1 mice ($F(5,27) = 5.890$, $p = 0.0008$). The TBARS content peaked at 70 weeks of age. The TBARS level at 70 weeks of age was 2.6-fold greater than that at 12 weeks of age. A two-way ANOVA showed a significant interaction between the effects of strain and age on the TBARS content ($F(1,15) = 11.044$, $p = 0.0046$). Simple main effects analysis showed that 70-week-old SAMP1 mice showed greater TBARS content than SAMR1 mice at the same age, whereas there were no differences between 12-week-old SAMP1 and SAMR1 mice (Fig. 8).

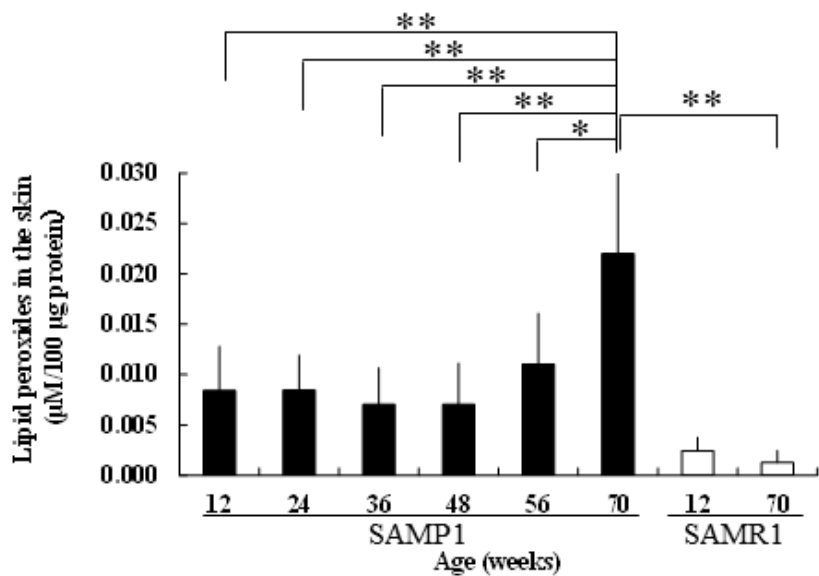


Fig. 8. Age-associated changes in the TBARS levels in the skin from SAMP1 and SAMR1 mice.

The TBARS levels in the skin from SAMP1 and SAMR1 mice were measured and normalized against the protein content of the homogenate. The closed bars represent SAMP1 mice, and the open bars represent SAMR1 mice. All data are presented as means \pm S.D. The number of mice used in this experiment ranged from 4 to 11 for each experimental group. (*) $p < 0.05$, (**) $p < 0.01$

Discussion

In the present study, I demonstrated that the age-associated histological and molecular expression changes in SAMP1 skin resembled those observed in human photoaged skin. Table 1 summarizes the histological changes in old SAMP1 skin, with reference to the histological characteristics of human photoaged and intrinsically aged skin. The histological changes in old SAMP1 mice share many features with human photoaging, rather than with intrinsic aging. In addition, skin from UV-irradiated hairless mice also exhibited similar histological changes [3].

Recent studies have revealed that UV irradiation to human skin induces transcriptional factor activator protein 1 (AP-1) and nuclear factor-kappa B (NF- κ B) upregulation [9]. AP-1 and NF- κ B stimulate the transcription of genes for matrix-degrading enzymes such as metalloproteinase and pro-inflammatory cytokine genes, respectively [9]. The expression changes of these genes are considered to be directly related to the pathogenesis of photoaged skin [31]. As presented in Fig. 4 to 7 and Table 2, the age-associated changes in the expression of these photoaging-associated molecules in SAMP1 skin were similar to those observed in human photoaged skin. The upregulation of pro-inflammatory cytokines, such as IL-1 β [32,33], TNF- α [34], IL-6 [35,36]

and IFN- γ [37], has been described in human photoaged skin. The age-associated upregulation of these cytokines has also been reported in the brain of old SAMP8 [38] and SAMP10 [29] mice. Thus, a shift to a pro-inflammatory status with advancing age may be a common phenomenon in the SAMP strains of mice. The enhanced expression of TGF- β 1 has been reported in UVB- and solar-simulated UV-exposed skin [39,40]. iNOS mRNA has been reported to be induced by UV exposure in human skin organ culture [41]. Nitric oxide, produced by iNOS, reacts with superoxide to form peroxynitrite, which then causes nitrosative damage to macromolecules. In fact, 3-nitrotyrosine is elevated in human photoaged skin [42]. MMPs are the main contributor to the alterations in the composition of the dermal matrix, which are the most conspicuous histological features of photoaged skin [1]. In the present study, I focused on MMP-7 and -12, since I found a prominent increase in elastic fibers in old SAMP1 skin. These MMPs have the capability to degrade elastin, and are considered to contribute to the remodeling of the elastotic areas in sun-damaged skin [43]. I found that both MMPs showed an age-associated upregulation in SAMP1 skin (Fig. 7), which is a common feature with human photoaged skin [43,44].

UV-induced ROS have been suggested to be a promoting factor for photoaging [9], and chronic UV exposure leads to increased levels of

mitochondrial DNA deletions in human skin [45]. The results in this study suggest that the increase in ROS production may be sufficient to induce photoaging-like phenotypes. SAMP1 mice strains have been used in numerous studies as a model for human geriatric disorders, and Hosokawa *et al.* previously proposed that they are a model of a spontaneously higher oxidative status, partly caused by mitochondrial dysfunction [19,24]. Increased TBARS levels in old SAMP1 skin (Fig. 8), and increased ROS production in dermal fibroblast-like cells from SAMP11 mice [23] indicate that the skin of old SAMP mice is under a higher oxidative environment. UV-induced ROS contribute to the pathogenesis of photoaging in humans, whereas ROS from defective mitochondria may be the culprit responsible for the aging phenotypes of old SAMP1 mice. Considering that ROS are at least a promoting factor for intrinsic aging, “extrinsic” photoaging might be explained as an exaggerated form of intrinsic aging.

In summary, the skin from old SAMP1 mice exhibited phenotypes closely resembling human photoaged skin, in terms of histological and molecular expression changes and increased oxidative stress. SAMP1 mice may be a useful spontaneous animal model for investigating the link among the intrinsic aging process, oxidative stress, and photoaging phenotypes, and in evaluating the efficacy of anti-photoaging therapy by topical and oral antioxidants [46].

Table 1

Anatomic comparison between the dorsal skin from old SAMP1 mice, human photoaged skin and intrinsically aged skin.

| | Dorsal skin from old SAMP1 mice | Human photoaged skin ^a | Human intrinsically aged skin ^a |
|---------------------------|--|--|--|
| Glycosaminoglycan | Markedly increased | Markedly increased | Slightly increased |
| Elastic fiber | Markedly increased; degenerates into amorphous | Markedly increased; degenerates into amorphous | Almost normal |
| Fibroblasts | Increased and hyperactive | Increased and hyperactive | Decreased and inactive |
| Mast cells | Increased | Increased | Decreased |
| Dermal-epidermal junction | Flattened | Flattened | Not flattened |
| Epidermal thickness | Thickened | Thickened | Thinned |
| Grenz zone | Prominent | Prominent | Absent |

^aModified from Refs. [2] and [3].

Table 2

Changes in mRNA expression in the dorsal skin from old SAMP1 mice and human photoaged skin.

| | Dorsal skin from old SAMP1 skin | Human photoaged skin | References |
|----------------|---------------------------------|----------------------|------------|
| IL-1 β | p = 0.0556 (\uparrow) | \uparrow | 32,33 |
| TNF- α | \uparrow | \uparrow | 34 |
| IL-6 | \uparrow | \uparrow | 35,36 |
| IFN- γ | \uparrow | \uparrow | 37 |
| TGF- β 1 | \uparrow | \uparrow | 39,40 |
| iNOS | \uparrow | \uparrow | 41 |
| MMP-7 | \uparrow | \uparrow | 42 |
| MMP-12 | \uparrow | \uparrow | 43 |

CHAPTER 2

**Differences in the histopathology and cytokine expression pattern
between chronological aging and photoaging of hairless mice skin**

Abstract

Skin photoaging is a complex, multifactorial process resulting in functional and structural changes of the skin, and different phenotypes from chronological skin aging are well-recognized. Ultraviolet (UV)-irradiated hairless mice have been used as a skin photoaging animal model. However, differences in morphology and gene expression patterns between UV-induced and chronological skin changes in this mouse model have not been fully elucidated. Here I investigated differences in histopathology and cytokine expression between UV-irradiated and non-irradiated aged hairless mice to clarify factor(s) that differentiate photoaging from chronological skin aging phenotypes. Eight-week-old HR-1 hairless mice were divided into UV-irradiated (UV-irradiated mice) and non-irradiated (control mice) groups. Irradiation was performed three times per week for 10 weeks. In addition, 30-week-old HR-1 hairless mice were reared until 70 weeks of age without UV irradiation (aged mice). Histopathologies revealed that the flattening of dermal-epidermal junctions and epidermal thickening were observed only in UV-irradiated mice. Decreases in fine elastic fibers just beneath the epidermis, the thickening of elastic fibers in the reticular dermis, and the accumulation of glycosaminoglycans were more prominent in UV-irradiated mice as compared to non-irradiated aged mice. Quantitative PCR analyses revealed that

UV-irradiated mice showed an increase in the expression of IFN- γ . In contrast, aged mice exhibited proportional upregulation of both pro-inflammatory and anti-inflammatory cytokines. The IFN- γ /IL-4 ratio, an indicator for the balance of pro-inflammatory and anti-inflammatory cytokines, was significantly higher in UV-irradiated mice as compared to control and non-irradiated aged mice. An elevated IFN- γ /IL-4 ratio was also observed in aged senescence-accelerated mouse-prone 1 (SAMP1) mice, a spontaneous skin photoaging model. Thus, an imbalance between pro-inflammatory and anti-inflammatory cytokines might be a key factor to differentiate photoaged skin from chronologically-aged skin.

Introduction

Studying the pathogenesis of photoaged skin in humans is difficult because of the decades needed for the evolution of this process, and the inability to assess the total exposure to UV in a given individual [47]. Therefore, UV-irradiated skh-hairless mice are widely used as an animal model for skin photoaging in the elderly [15]. In this model, UV irradiation generally starts at 6 to 8 weeks of age, and 10 to 22 weeks of irradiation are sufficient to produce human photoaged skin-like lesions [16,17]. In other words, photoaged skin-like lesions are developed at an adult age, but not in aged hairless mice; thus, an intrinsic senescence process, which is essential for the manifestation of the phenotype of photoaged skin in humans, seems to be unnecessary to reproduce the photoaged skin-like lesions in hairless mice. These experimental conditions resulted in a paucity of studies that have addressed chronological skin changes in hairless mice.

Kligman *et al.*, reported that skin from hairless mice at an advanced (80-week-old) age without UV irradiation exhibited a sparse distribution of elastic fibers in the dermis, and flocculent deposits of glycosaminoglycans (GAGs) in the dermal-epidermal junctions (DEJ) [48]. These histological changes were similar to chronologically-aged skin in photo-protected areas. Peres

et al., reported that there were quantitative and qualitative differences in oxidative stress generated by chronological aging versus photoaging of hairless mice [49]. The skin is intensively subjected to exogenous and endogenous assaults; consequently, mechanisms concerning chronological aging and photoaging remained to be elucidated.

In this chapter, I describe an attempt to investigate differences in the histopathology and cytokine expression of non-irradiated skin at an advanced age (70 weeks of age), and UV-irradiated and non-irradiated skin at a young age (18 weeks of age) in hairless mice to clarify factor(s) that differentiate photoaging from chronological aging phenotypes in the skin.

Materials and Methods

Animals

Male albino hairless HOS: HR-1 hairless mice (6 weeks or 30 weeks of age) were purchased from Hoshino Laboratory Animals Co., Ltd. (Saitama, Japan). Mice were reared under conventional conditions, housed at $23 \pm 2^\circ\text{C}$, and were allowed free access to food (CE2, Nihon CLEA, Tokyo, Japan) and tap water. The light-dark cycle was set at 12 hours (lights were on at 07:00). Six-week-old male hairless mice were acclimated for 2 weeks in the animal facility of Institute for Developmental Research, Aichi Human Service Center, after which they were subjected to UV irradiation. They were divided into UV-irradiated ($n = 4$) and non-irradiated (control) ($n = 4$) groups. Thirty-week-old male hairless mice were reared until 70 weeks of age without UV irradiation (aged mice) ($n = 5$). I checked all of the mice pathologically after sampling of skin specimens, and excluded samples from mice with inflammation-associated pathologies (pneumonia and other inflammatory changes) and/or tumors from all subsequent analyses.

I took special care to minimize the number of animals used and their suffering. All animals were handled in accordance with the Guide for the Care and Use of Laboratory Animal of the Institute for Developmental Research, Aichi Human Service Center.

UVB irradiation

UV irradiation was performed according to a method described by Schwartz *et al.*, [50] with some modifications. Briefly, a Handheld UV Lamp UVM-57 (UVP Inc., CA, USA) was used as a source of UVB. The wavelength of the irradiated UV was 280-315 nm. A mouse was placed in a cage ($12 \times 9 \times 3$ cm) and positioned at the center of the UVB source. The cage was covered by thin wire netting such that the mice were evenly exposed to the UV. The UV intensity was measured using a UV radiometer YK-34UV (Lutron Electronic Co., Taipei, Taiwan) with spectral sensitivity within the range of 290-390 nm. The dorsal skin of the mice was irradiated three times per week for 10 weeks. The total irradiated dose was about 4 J/cm^2 . Skin tissues were removed two days after the completion of the UV irradiation.

Histological examinations

Each mouse was sacrificed by cervical dislocation, and the dorsal skin was rapidly removed, immersed in 10% neutral buffered formalin (pH 7.4) for 7 days, and then embedded in paraffin. Twenty-micron-thick sections were cut with a sliding microtome, and hematoxylin-eosin (H&E), resorcin-fuchsin and alcian blue stainings were performed according to standard procedures.

The thickness of the epidermis was evaluated using sections stained with H&E. Photomicrographs of continuous, non-overlapping visual fields ($736 \times 533 \mu\text{m}$) were obtained to cover the entire epidermis of the specimen using a digital microscope (VHX-200, Keyence Corporation, Osaka, Japan). The thickness of the epidermis was measured at 10 locations set at an interval of $70 \mu\text{m}$ apart, and the average thickness was calculated.

RNA extraction and real-time quantitative PCR

Dorsal skin was dissected from each mouse, and washed in ice-cold phosphate-buffered saline (PBS). Total RNA was isolated using an ISOGEN kit (NIPPON GENE CO., LTD., Tokyo, Japan) according to the manufacturer's instructions. RNA yields and purities were determined by spectrophotometric absorption analyses at 260/280 nm. The cDNA was synthesized from total RNA using the SuperScriptTM III First-Strand Synthesis System for RT-PCR (Invitrogen, Carlsbad, CA, USA) according to the manufacturer's instructions.

Gene expression was analyzed by a real time (RT) PCR system (ABI Stepone-Plus, Applied Biosystems, Foster City, CA, USA) with each cDNA sample, specific Taqman primers/probes and a Taqman Universal PCR Master Mix (Applied Biosystems, Foster City, CA, USA). The following probes were used (identified by Applied Biosystems assay identification number): IL-1 beta

(IL-1 β), Mm00434228_m1; TNF-alpha (TNF- α), Mm00443258_m1; IL-6, Mm00446190_m1; IFN-gamma (IFN- γ), Mm00801778_m1; TGF-beta1 (TGF- β 1), Mm00441724_m1; iNOS, Mm00440485_m1; IL-4, Mm00445260_m1; IL-10, Mm00439616_m1 and 18S rRNA, Hs99999901_s1.

18S rRNA was used as an internal control. The expression of these mRNA species was analyzed using the same sets as for the total RNA samples. Reaction mixtures were subjected to the following amplification scheme: 1 cycle at 50 °C for 2 min (AmpErase uracil-N-glycosylase deactivation) and 1 cycle at 95 °C for 10 min (AmpliTaq Gold activation), followed by 40 cycles at 95 °C for 15 s (denaturation) and 60 °C for 1 min (annealing and extension).

Statistical Analyses

Data were expressed as means \pm S.D. A one-way analysis of variance (ANOVA) followed by Tukey's procedure were performed to determine differences in epidermal thickness and the expression of mRNA among control, aged and UV-irradiated groups of hairless mice. Differences were considered to be statistically significant when $p < 0.05$.

Results

Histological analyses

In H&E-stained sections, spike-like downgrowths in the area of the DEJ were evident in both control and aged mice (Fig. 9a, b). In contrast, UV-irradiated mice showed an increase in the area of flattened DEJ (Fig.9c). UV-irradiated mice, but not aged mice, showed marked thickening of the epidermis (Fig. 9a, b, c). A one-way ANOVA showed a significant effect for aging type ($F(2,10) = 50.6086$, $p < 0.0001$) in the epidermal thickness. Post-hoc analyses revealed that the thickness of UV-irradiated mice epidermis ($38.80 \pm 5.85 \mu\text{m}$) was significantly thicker than that in control mice ($17.21 \pm 1.54 \mu\text{m}$) and that in aged mice ($16.38 \pm 2.42 \mu\text{m}$). In contrast, there were no significant differences between control and aged mice.

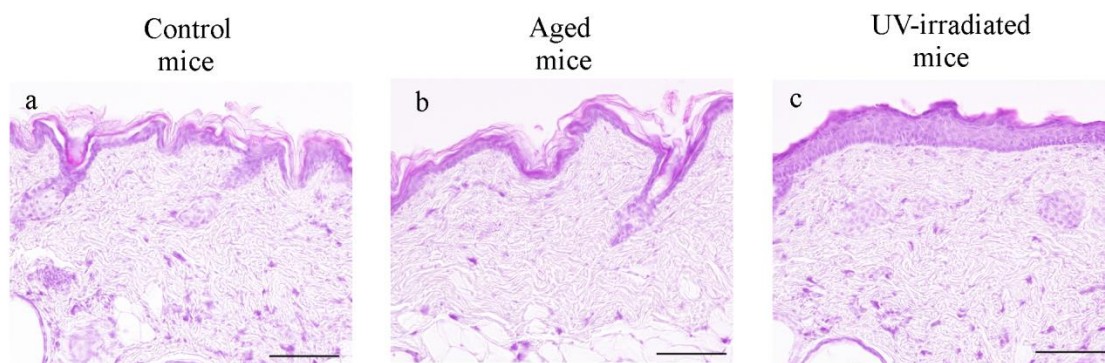


Fig. 9. Histological changes in the dorsal skin of hairless mice revealed by hematoxylin and eosin (H&E) staining.

Representative photomicrographs of the dorsal skin from control (a), aged (b) and UV-irradiated (c) hairless mice. Formalin-fixed skin sections were stained with H&E. Photomicrographs were taken with a reduced condenser aperture. See the text for a detailed description. Scale bars: 100 μm .

In resorcin-fuchsin-stained sections, fine elastic fibers just beneath the epidermis were fewer in aged mice (Fig.10a, b, open arrowheads). The elastic fibers in the reticular dermis were thickened in aged mice as compared to control mice (Fig. 10b, thin arrow). In the UV-irradiated mice, the above mentioned changes were more pronounced as compared to control mice (Fig. 10c, open arrowhead and thin arrow).

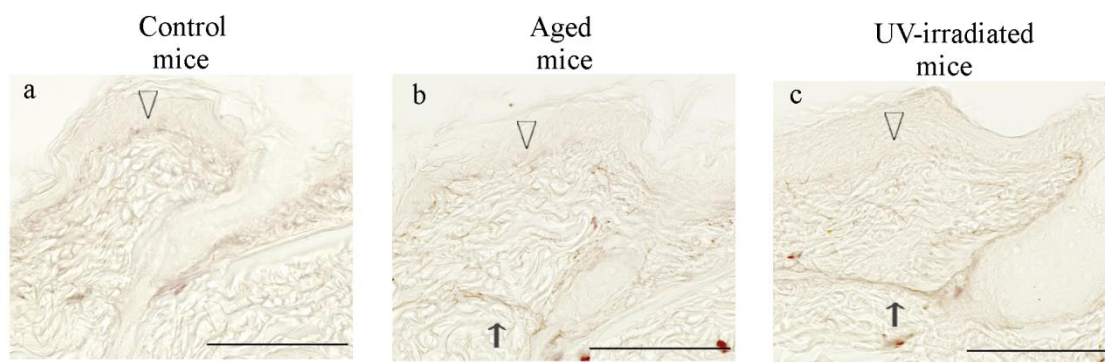


Fig. 10. Histological changes in the dorsal skin of hairless mice revealed by resorcin-fuchsin staining.

Representative photomicrographs of the dorsal skin from control (a), aged (b) and UV-irradiated (c) hairless mice. Formalin-fixed skin sections were stained with resorcin-fuchsin. The open arrowheads indicate fine elastic fibers in the dermal-epidermal junction, and the thin arrows indicate thickened elastic fibers in the reticular dermis. Photomicrographs were taken with a reduced condenser aperture. See the text for a detailed description. Scale bars: 100 μm .

In alcian blue-stained sections, a slight accumulation of alcian blue-positive GAGs was observed just beneath the epidermis of aged mice (Fig. 11b, closed arrowheads). The UV-irradiated mice showed a more prominent accumulation of GAGs just beneath the epidermis (Fig. 11c, closed arrowheads).

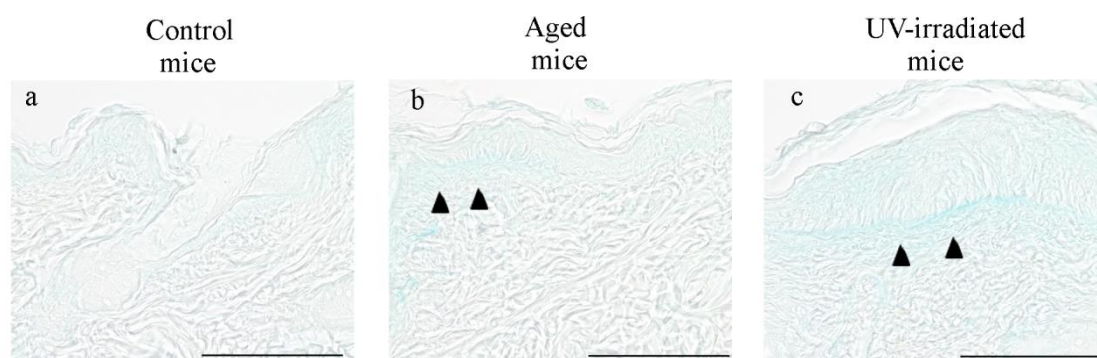


Fig. 11. Histological changes in the dorsal skin of hairless mice revealed by alcian blue staining.

Representative photomicrographs of the dorsal skin from control (a), aged (b) and UV-irradiated (c) hairless mice. Formalin-fixed skin sections were stained with alcian blue. The closed arrowheads in (b) and (c) indicate increased glycosaminoglycans. Photomicrographs were taken with a reduced condenser aperture. See the text for a detailed description. Scale bars: 100 μm .

Gene expression analyses of hairless mouse skin by real-time PCR

A one-way ANOVA revealed no significant effect for aging type (control, UV-irradiated and chronologically-aged) in the expression of IL-1 β mRNA ($F(2,10) = 1.0554$, $p = 0.3838$) (Fig. 12a).

In the expression of TNF- α mRNA, a one-way ANOVA showed a significant effect for the aging type ($F(2,10) = 8.3231$, $p = 0.0074$). TNF- α mRNA expression in aged mice was significantly greater than in control and UV-irradiated mice, whereas there was no significant difference between control and UV-irradiated mice (Fig. 12b).

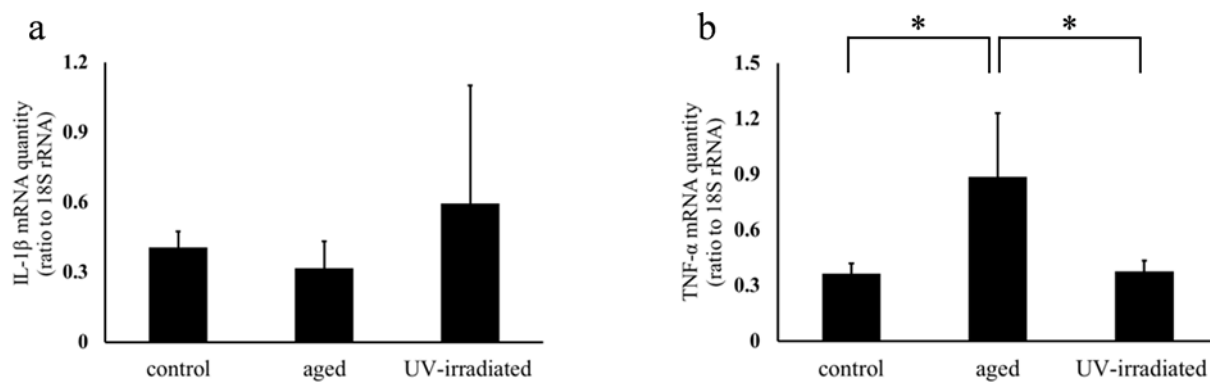


Fig. 12. Changes in the expression of IL-1 β and TNF- α mRNA in the skin from hairless mice. The expression of IL-1 β (a) and TNF- α (b) mRNAs in the skin from control, aged and UV-irradiated hairless mice were analyzed by real-time PCR. The relative levels of mRNA were obtained by dividing the quantity of each mRNA by that of 18S rRNA as the internal standard. All data are presented as means \pm S.D. The number of mice used in this experiment ranged from 4 to 5 for each experimental group. (*) $p < 0.05$.

A one-way ANOVA revealed no significant effect for aging type (control, UV-irradiated and chronologically-aged) in the expression of IL-6 mRNA ($F(2,10) = 2.8796$, $p = 0.1029$) (Fig. 13a).

In the expression of IFN- γ mRNA, a one-way ANOVA showed a significant effect for the aging type ($F(2,10) = 12.0917$, $p = 0.0021$). Tukey's procedure revealed significantly greater IFN- γ mRNA expression in UV-irradiated mice as compared to control (5.8-fold) and aged (2.0-fold) mice (Fig. 13b).

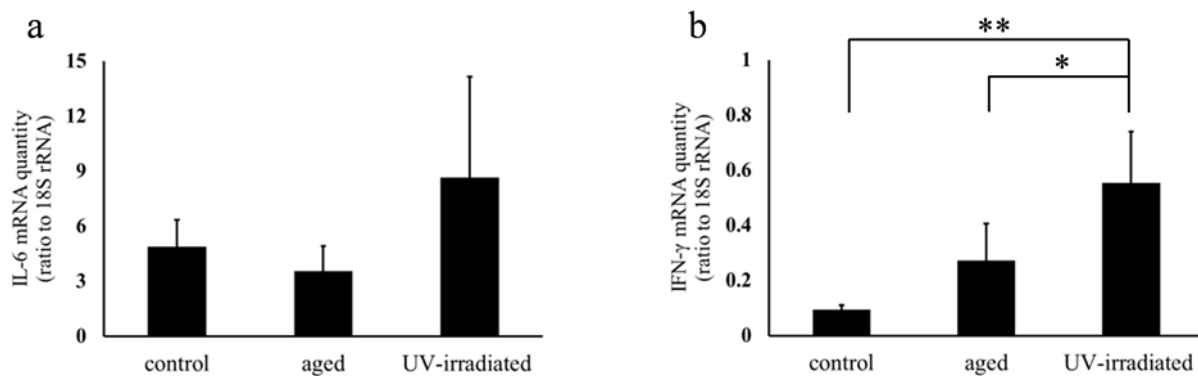


Fig. 13. Changes in the expression of IL-6 and IFN- γ mRNA in the skin from hairless mice. The expression of IL-6 (a) and IFN- γ (b) mRNAs in the skin from control, aged and UV-irradiated hairless mice were analyzed by real-time PCR. The relative levels of mRNA were obtained by dividing the quantity of each mRNA by that of 18S rRNA as the internal standard. All data are presented as means \pm S.D. The number of mice used in this experiment ranged from 4 to 5 for each experimental group. (*) $p < 0.05$, (**) $p < 0.01$.

In the expression of TGF- β 1 mRNA, a one-way ANOVA showed a significant effect for the aging type ($F(2,10) = 29.3000$, $p = 0.0001$). TGF- β mRNA levels in aged mice were significantly greater than those in control and UV-irradiated mice. No significant differences were detected between control and UV-irradiated mice (Fig. 14a).

In the expression of iNOS mRNA, a one-way ANOVA showed a significant effect for the aging type ($F(2,10) = 23.4744$, $p = 0.0002$). iNOS mRNA levels in aged mice were significantly greater than those in control and UV-irradiated mice. No significant differences were detected between control and UV-irradiated mice (Fig. 14b).

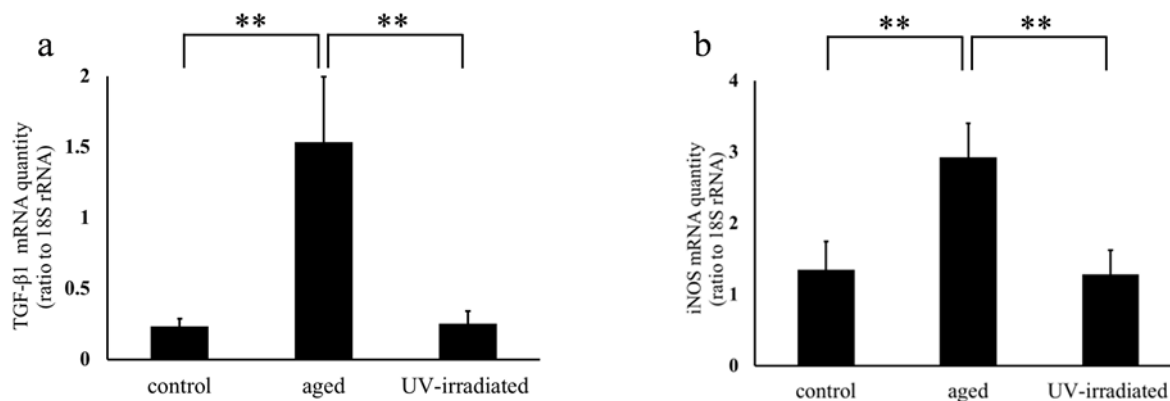


Fig. 14. Changes in the expression of TGF-β1 and iNOS mRNA in the skin from hairless mice.

The expression of TGF-β1 (a) and iNOS (b) mRNAs in the skin from control, aged and UV-irradiated hairless mice were analyzed by real-time PCR. The relative levels of mRNA were obtained by dividing the quantity of each mRNA by that of 18S rRNA as the internal standard. All data are presented as means \pm S.D. The number of mice used in this experiment ranged from 4 to 5 for each experimental group. (**) $p < 0.01$.

In the expression of IL-4 mRNA, a one-way ANOVA showed a significant effect for the aging type ($F(2,10) = 5.0001$, $p = 0.0312$). IL-4 mRNA levels in aged mice were 3.3-fold higher than those in control mice. In contrast, no significant differences were detected between control and UV-irradiated mice (Fig. 15a).

In the expression of IL-10, a one-way ANOVA showed a significant effect for the aging type ($F(2,10) = 6.7659$, $p = 0.0139$). IL-10 mRNA levels in aged mice were 3.4-fold greater than those in control mice. In contrast, no significant differences were detected between control and UV-irradiated mice (Fig. 15b).

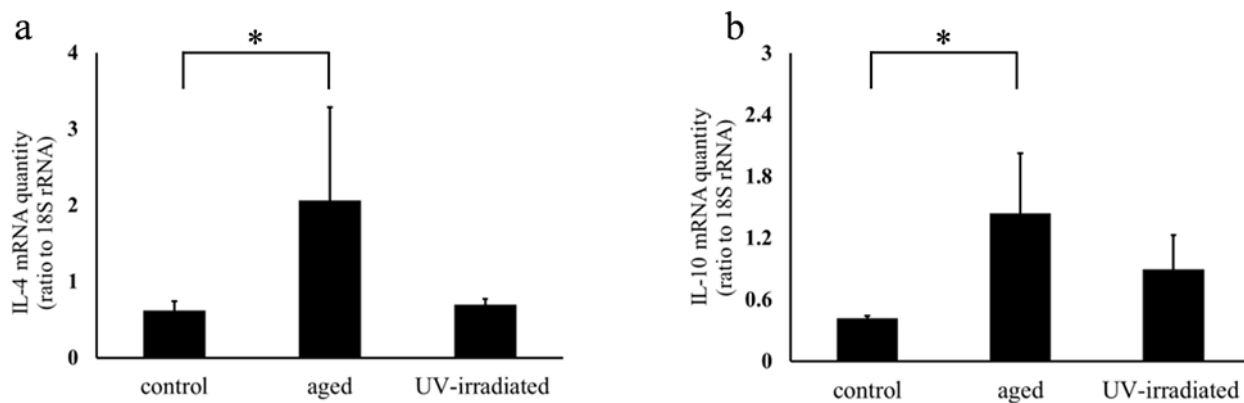


Fig. 15. Changes in the expression of IL-4 and IL-10 mRNA in the skin from hairless mice. The expression of IL-4 (a) and IL-10 (b) mRNAs in the skin from control, aged and UV-irradiated hairless mice were analyzed by real-time PCR. The relative levels of mRNA were obtained by dividing the quantity of each mRNA by that of 18S rRNA as the internal standard. All data are presented as means \pm S.D. The number of mice used in this experiment ranged from 4 to 5 for each experimental group. (*) $p < 0.05$.

To evaluate the balance between pro-inflammatory and anti-inflammatory cytokines, I compared the IFN- γ /IL-4 ratio among control, aged and UV-irradiated mice (Fig. 16). A one-way ANOVA showed a significant effect for the aging type ($F(2,10) = 40.6563$, $p < 0.0001$). The IFN- γ /IL-4 ratio was significantly greater in UV-irradiated mice than in control and aged mice. In contrast, there was no significant difference in the IFN- γ /IL-4 ratio between control and aged mice (Fig. 16).

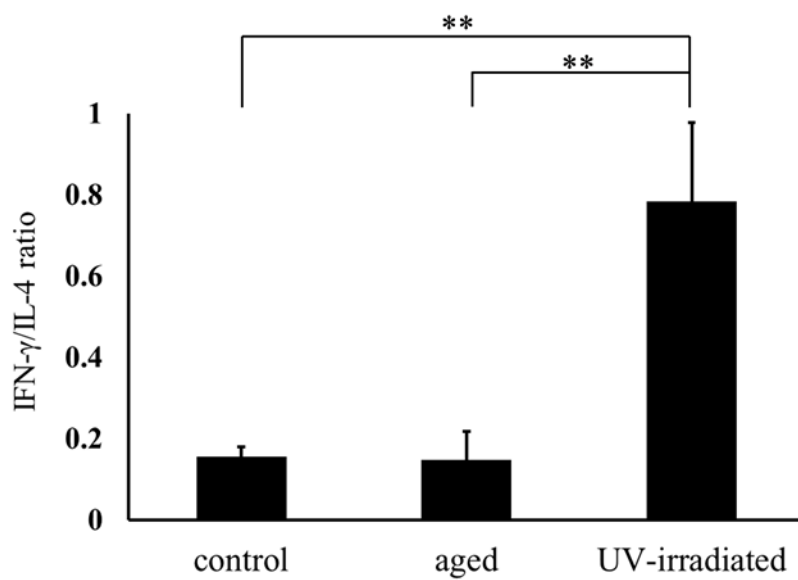


Fig. 16. Changes in the IFN- γ /IL-4 ratio in the skin from hairless mice. The IFN- γ /IL-4 ratio from control, aged and UV-irradiated hairless mice were indicated. All data are presented as means \pm S.D. The number of mice used in this experiment ranged from 4 to 5 for each experimental group. (**) $p < 0.01$.

To evaluate whether the imbalance between pro-inflammatory and anti-inflammatory cytokines may contribute to the pathogenesis of photoaged skin phenotype, I compared the IL-4 mRNA expression and IFN- γ /IL-4 ratio in the skin from SAMP1 mice, a spontaneous photoaging model, and control SAMR1 mice.

In the expression of IL-4 mRNA, a one-way ANOVA showed a significant effect for age in SAMP1 mice ($F(5,28) = 9.6324$, $p < 0.0001$). The expression of IL-4 mRNA increased dramatically towards 48 weeks of age, but then decreased at 70 weeks of age. The expression level of IL-4 mRNA at 48 weeks of age was about 10-fold higher than that at 12 weeks of age. A two-way ANOVA showed a significant interaction between the effects of strain and age on the expression of IL-4 ($F(1,14) = 13.1949$, $p = 0.0027$). Simple main effects analysis revealed that 70-week-old SAMR1 mice showed greater expression than that in SAMP1 mice at the same age, whereas there were no differences between 12-week-old SAMP1 and SAMR1 mice (Fig. 17a).

In the ratio of IFN- γ /IL-4, a one-way ANOVA showed a significant effect for age in SAMP1 mice ($F(5,28) = 41.8817$, $p < 0.0001$). The IFN- γ /IL-4 ratio at 70 weeks of age was 107.5-fold higher than that at 12 weeks of age. A two-way ANOVA showed a significant interaction between

the effects of strain and age on the IFN- γ /IL-4 ratio ($F(1,14) = 28.4944$, $p = 0.0001$). Simple main effects analysis revealed that 70-week-old SAMP1 mice showed greater IFN- γ /IL-4 ratio than that in SAMR1 mice at the same age, whereas there were no differences between 12-week-old SAMP1 and SAMR1 mice (Fig. 17b).

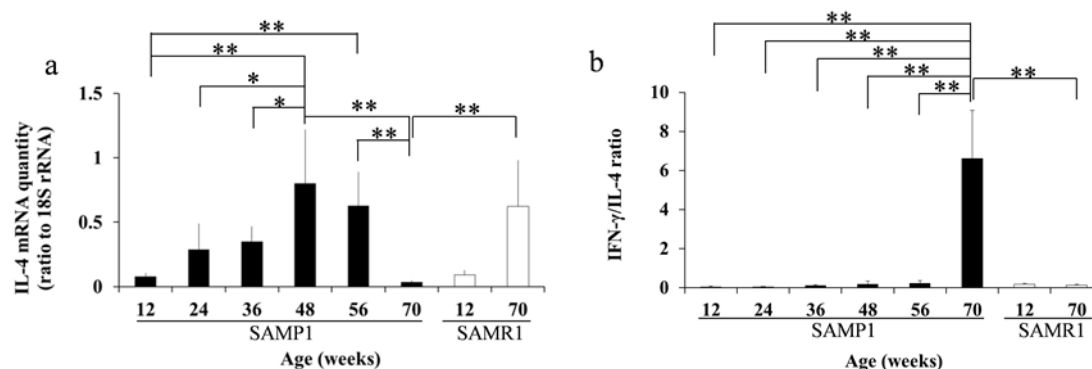


Fig. 17. Expression changes in IL-4 mRNA and IFN- γ /IL-4 ratio in the skin from SAMP1 and SAMR1 mice.

The expression of IL-4 mRNA (a) in the skin from SAMP1 and SAMR1 mice were analyzed by real-time PCR. The relative levels of mRNA were obtained by dividing the quantity of each mRNA by that of 18S rRNA as the internal standard. (b) indicates IFN- γ /IL-4 ratio. The closed bars represent SAMP1 mice, and the open bars represent SAMR1 mice. All data are presented as means \pm S.D. The number of mice used in this experiment ranged from 4 to 11 for each experimental group. For the detailed materials and methods, see chapter 1. (*) $p < 0.05$, (**) $p < 0.01$.

Discussion

In the present study, I showed that aged (70-week-old) hairless mice exhibited minimal changes in their dermal elastic fibers and GAGs without epidermal thickening. These changes were similar to those in a previous report by Kligman *et al.*, [48] and to the pathology of chronologically-aged skin in photo-protected areas in humans, except for the absence of flattening of DEJ [11]. In contrast, I were able to reproduce photoaging-like histological changes, such as alterations in dermal elastic fibers, the deposition of GAG and thickening of the epidermis [2,3], in hairless mice by UV irradiation for 10 weeks. Thus, chronological factors may have little, if any, contribution to the pathogenesis of the photoaging-like phenotype in hairless mice, and UV irradiation seems to be a necessary and sufficient factor.

ROS, pro-inflammatory cytokines and MMPs are thought to be key factors for the pathogenesis of photoaging [1,9]. On the other hand, these factors also contribute to the intrinsic aging process of the skin [51-53]. Accumulating evidence suggests that photoaging and chronological aging share some important molecular features, and photoaging can be regarded as the superposition of solar damage on the normal aging process [2,53]. To investigate differentiating molecular factor(s) between photoaging and

chronological aging, I focused on the pattern of cytokine expression in hairless mice models for these two aging phenotypes. I found that chronologically aged hairless mice showed an increase in the expression of both pro-inflammatory molecules, such as TNF- α and iNOS, and anti-inflammatory molecules, such IL-4 and IL-10. In contrast, UV-irradiated hairless mice showed a marked increase in IFN- γ expression, but no significant increase in anti-inflammatory cytokines. A balanced production of pro-inflammatory and anti-inflammatory cytokines is important for an appropriate immune response [54-56], and an imbalance between pro-inflammatory and anti-inflammatory cytokines has been reported in psoriasis, a chronic inflammatory skin disease caused by autoimmune mechanisms [57]. To evaluate the balance between pro-inflammatory and anti-inflammatory cytokines in these two aging phenotypes, I calculated the IFN- γ /IL-4 ratio [54,58]. In chronologically-aged skin, the IFN- γ /IL-4 ratio was similar to that in control mice, suggesting that the pro-inflammatory/anti-inflammatory balance is maintained in aged hairless mice. In contrast, UV-irradiated hairless mice showed a significant increase in their IFN- γ /IL-4 ratio. Thus, although not all pro-inflammatory cytokines were increased in UV-irradiated mice, the imbalance between pro-inflammatory versus

anti-inflammatory cytokines might be a differentiating factor between the two aging phenotypes in the skin.

To confirm the association between the skin photoaging phenotype and the shift to pro-inflammatory status, I evaluated the IFN- γ /IL-4 ratio in SAMP1 mice (Fig. 17b). The IFN- γ /IL-4 ratio of the skin from 70-week-old SAMP1 mice was markedly increased as compared to that of 12-week-old SAMP1 mouse skin. In contrast, no significant difference was observed between 12- and 70-weeks of age the IFN- γ /IL-4 ratios in SAMR1 mice. Thus, the imbalance between pro-inflammatory and anti-inflammatory cytokines seems to be a common feature of UV-irradiated hairless mice and old SAMP1 mice, which are both skin photoaging models.

Conclusion

Based on the results of this study, a SAMP1 strain of mice with a higher oxidative status is proposed as a new animal model for human skin photoaging due to exaggerated intrinsic factors. The skin from old SAMP1 mice exhibited phenotypes closely resembling human photoaged skin, in terms of histological changes, the expression changes of cytokines and MMPs. Several antioxidants are available in topical and oral preparations to prevent or treat photoaging [46]. Since SAMP1 mice are a unique model which develops photoaging-like phenotypes due to higher oxidative stress, the effects of antioxidants may be observed more clearly than in an UV-irradiation model. The SAMP1 mouse strain can be a useful spontaneous animal model for investigating the pathogenic mechanisms of human photoaging, especially the mechanistic link among the intrinsic aging process, oxidative stress and photoaging phenotypes.

An attempt was made to clarify factor(s) that differentiate photoaging from chronological aging phenotypes. Histological changes were compared with cytokine expression patterns among UV-irradiated hairless mice (18 weeks of age), a standard photoaging model, non-irradiated mice of 18 weeks of age and chronologically-aged hairless mice (70 weeks of age).

Chronologically-aged skin and photoaged skin in hairless mice exhibited different histological and gene expression changes, and an imbalance between pro-inflammatory and anti-inflammatory cytokines, indicated by an elevated IFN- γ /IL-4 ratio, which might be a key factor to differentiate these two phenotypes of skin aging. Interestingly, SAMP1 mice also showed increased IFN- γ /IL-4 ratio with advancing age. Finally, an imbalance between pro-inflammatory and anti-inflammatory conditions caused by UV and/or ROS is proposed as a mechanism of skin photoaging. How the pro-inflammatory/anti-inflammatory imbalance affects phenotypes of photoaged skin deserves further investigation. These novel results contribute towards the fundamental understanding of the regulatory mechanisms of photoaged skin and chronologically-aged skin in photo-protected skin. These results can help determine if photoaging is a pathological process or part of the normal aging process.

Acknowledgments

I thank Professor Minoru Takeuchi for his guidance and encouragement throughout this work. I wish to thank Dr. Masanori Hosokawa, Dr. Yoichi Chiba, Dr. Yasushi Enokido and Dr. Ayako Furukawa for their suggestions and excellent technical helps in this study. I also thank Ms. Noriko Kawamura, Ms. Tomoko Kitajima, Ms. Takae Hiraide and Ms. Emi Kamiya for their technical assistance. In the last, I would like to express my sincere thanks to the members in our company for their encouragements and valuable suggestions.

References

- [1] Rabe J H, Mamelak A J, McElgunn P J S, Morison W L, Sauder D N. Photoaging: mechanisms and repair. *J Am Acad Dermatol* 2006; 55: 1-19.
- [2] Farage M A, Miller K W, Elsner P, Maibach H I. Intrinsic and extrinsic factors in skin ageing: a review. *Int J Cosmet Sci* 2008; 30: 87-95.
- [3] Kligman L H, Kligman A M. The nature of photoaging: its prevention and repair. *Photodermatol* 1986; 3: 215-227.
- [4] Berneburg M, Plettenberg H, Krutman J. Photoaging of human skin. *Photodermatol Photoimmunol Photomed* 2000; 16: 239-244.
- [5] Epstein J H. Photocarcinogenesis, skin cancer, and aging. In: Balin A K, Kligman A M, eds. *Aging and the skin*. New York: Raven Press, 1989: 307-329.
- [6] Sugimoto M, Yamashita R, Ueda M. Telomere length of the skin in association with chronological aging and photoaging. *J Dermatol Sci* 2006; 43: 43-47.
- [7] Svobodová A, Psotová J, Walterová D. Natural phenolics in the prevention of UV-induced skin damage. A review. *Biomed Papers* 2003; 147: 137-145.
- [8] Kulka M. Mechanisms and treatment of photoaging and photodamage. In: Kulka M, eds. *Using old solutions to new problem – natural drug discovery in the 21st century*. InTech, 2013: 255-276.
- [9] Yaar M, Gilchrest B A. Photoageing: mechanism, prevention and therapy. *Br J Dermatol* 2007; 157: 874-887.
- [10] Rijken F, Bruijnzeel P L. The pathogenesis of photoaging: the role of neutrophils and neutrophil-derived enzymes. *J Investig Dermatol Symp Proc* 2009; 14: 67-72.
- [11] Mukherjee S, Date A, Patravale V, Korting H C, Roeder A, Weindl G. Retinoids in the treatment of skin aging: an overview of clinical efficacy and safety. *Clin Interv Aging* 2006; 1: 327-348.

- [12] Werth B B, Bashir M, Chang L, Werth V P. Ultraviolet irradiation induces the accumulation of chondroitin sulfate, but not other glycosaminoglycans, in human skin. *PLoS One* 2011; 6: e14830. doi:10.1371/journal.pone.0014830.
- [13] Lee J Y, Kim Y K, Seo J Y *et al.* Loss of elastic fibers causes skin wrinkles in sun-damaged human skin. *J Dermatol Sci* 2008; 50: 99-107.
- [14] Yaar M. Clinical and histological features of intrinsic versus extrinsic skin aging. In: Gilchrist B A, Krutmann J, eds. *Skin Aging*. Heidelberg: Springer-Verlag, 2006: 9-22.
- [15] Benavides F, Oberyszyn T M, VanBuskirk A M, Reeve V E, Kusewitt D F. The hairless mouse in skin research. *J Dermatol Sci* 2009; 53: 10-18.
- [16] Inomata S, Matsunaga Y, Amano S *et al.* Possible involvement of gelatinases in basement membrane damage and wrinkle formation in chronically ultraviolet B-exposed hairless mouse. *J Invest Dermatol* 2003; 120: 128-134.
- [17] Ropke C D, Sawada T C, da Silva V V, Michalany N S, de Moraes Barros S B. Photoprotective effect of *Pothomorpheumbellata* root extract against ultraviolet radiation induced chronic skin damage in the hairless mouse. *Clin Exp Dermatol* 2005; 30: 272-276.
- [18] Chiba Y, Fujisawa H, Nishikawa T, Hosokawa M. Higher oxidative stress status and mitochondrial alterations as a possible mechanism for senescence acceleration. In: Takeda T, Akiguchi I, Higuchi K, Hosokawa M, Hosokawa T, Nomura Y, eds. *The senescence-accelerated mouse (SAM): achievements and future directions*. Amsterdam: Elsevier, 2013: 373-387.
- [19] Chiba Y, Shimada A, Kumagai N *et al.* The senescence-accelerated mouse (SAM): a higher oxidative stress and age-dependent degenerative diseases model. *Neurochem Res* 2009; 34: 679-687.

- [20] Nomura Y, Takeda T, Okuma Y. 2004. The senescence-accelerated mouse (SAM): An animal model of senescence. Amsterdam: Elsevier.
- [21] Takeda T, Hosokawa M, Takeshita S *et al.* A new murine model of accelerated senescence. *Mech Ageing Dev* 1981; 17: 183-194.
- [22] Takeda T. Senescence-accelerated mouse (SAM): a biogerontological resource in aging research. *Neurobiol Aging* 1999; 20: 105-110.
- [23] Chiba Y, Yamashita Y, Ueno M *et al.* Cultured murine dermal fibroblast-like cells from senescence-accelerated mice as in vitro models for higher oxidative stress due to mitochondrial alterations. *J Gerontol A Biol Sci Med Sci* 2005; 60: 1087-1098.
- [24] Hosokawa M. A higher oxidative status accelerates senescence and aggravates age-dependent disorders in SAMP strains of mice. *Mech Ageing Dev* 2002; 123: 1553-1561.
- [25] Hosokawa M, Ashida Y, Nishikawa T, Takeda T. Accelerated aging of dermal fibroblast-like cells from senescence-accelerated mouse (SAM). 1. Acceleration of population aging in vitro. *Mech Ageing Dev* 1994; 74: 65-77.
- [26] Fujisawa H, Nishikawa T, Zhu B H *et al.* Aminoguanidine supplementation delays the onset of senescence in vitro in dermal fibroblast-like cells from senescence-accelerated mice. *J Gerontol A Biol Sci Med Sci* 1995; 54: 276-282.
- [27] Komura S, Yoshino K, Kondo K, Yagi K. Lipid peroxide levels in the skin of the senescence-accelerated mouse. *J Clin Biochem Nutr* 1988; 5: 255-260.
- [28] Okada T, Hayakawa R, Yoshino K *et al.* Deposition of lipofuscin and elastic fibers in the skin of the senescence-accelerated mouse. *J Clin Biochem Nutr* 1990; 9: 171-177.
- [29] Kumagai N, Chiba Y, Hosono M *et al.* Involvement of pro-inflammatory cytokines and microglia in an age-associated neurodegeneration model, the SAMP10 mouse. *Brain Res* 2007; 1185: 75-85.

- [30] Ohkawa H, Ohishi N, Yagi K. Assay for lipid peroxides in animal tissues by thiobarbituric acid reaction. *Anal Biochem* 1979; 95: 351-358.
- [31] Pillai S, Oresajo C, Hayward J. Ultraviolet radiation and skin aging: roles of reactive oxygen species, inflammation and protease activation, and strategies for prevention of inflammation-induced matrix degradation- a review. *Int J Cosmet Sci* 2005; 27: 17-34.
- [32] Takashima A, Bergstresser P R. Impact of UVB radiation on the epidermal cytokine network. *Photochem Photobiol* 1996; 63: 397-400.
- [33] Kupper T S, Chua A O, Flood P, McGuire J, Gubler U. Interleukin 1 gene expression in cultured human keratinocytes is augmented by ultraviolet irradiation. *J Clin Invest* 1987; 80: 430-436.
- [34] Köck A, Schwarz T, Kirnbauer R *et al.* Human keratinocytes are a source for tumor necrosis factor α : evidence for synthesis and release upon stimulation with endotoxin or ultraviolet light. *J Exp Med* 1990; 172: 1609-1614.
- [35] de Vos S, Brach M, Budnik A, Grewe M, Herrmann F, Krutmann J. Post-transcriptional regulation of interleukin-6 gene expression in human keratinocytes by ultraviolet B radiation. *J Invest Dermatol* 1994; 103: 92-96.
- [36] Urbanski A, Schwarz T, Neuner P *et al.* Ultraviolet light induces increased circulating interleukin-6 in humans. *J Invest Dermatol* 1990; 94: 808-811.
- [37] Terui T, Tagami H. Mediators of inflammation involved in UVB erythema. *J Dermatol Sci* 2000; 23 (Suppl 1): S1-5.
- [38] Tha K K, Okuma Y, Miyazaki H *et al.* Changes in expressions of pro-inflammatory cytokines IL-1 β , TNF- α and IL-6 in the brain of senescence accelerated mouse (SAM) P8. *Brain Res* 2000; 885: 25-31.

- [39] Wang H, Kochevar I E. Involvement of UVB-induced reactive oxygen species in TGF- β biosynthesis and activation in keratinocytes. *Free Radic Biol Med* 2005; 38: 890-897.
- [40] Quan T, He T, Kang S, Voorhees J J, Fisher G J. Ultraviolet irradiation alters transforming growth factor β /smad pathway in human skin in vivo. *J Invest Dermatol* 2002; 119: 499-506.
- [41] Suschek C V, Bruch-Gerharz D, Kleinert H, Förstermann U, Kolb-Bachofen V. Ultraviolet A₁ radiation induces nitric oxide synthase-2 expression in human skin endothelial cells in the absence of pro-inflammatory cytokines. *J Invest Dermatol* 2001; 117: 1200-1205.
- [42] Nishigori C, Hattori Y, Arima Y, Miyachi Y. Photoaging and oxidative stress. *Exp Dermatol* 2003; 12 (Suppl 2): 18-21.
- [43] Saarialho-Kere U, Kerkelä E, Jeskanen L *et al.* Accumulation of matrilysin (MMP-7) and macrophage metalloelastase (MMP-12) in actinic damage. *J Invest Dermatol* 1999; 113: 664-672.
- [44] Vaalamo M, Kariniemi A L, Shapiro S D, Saarialho-Kere U. Enhanced expression of human metalloelastase (MMP-12) in cutaneous granulomas and macrophage migration. *J Invest Dermatol* 1999; 112: 499-505.
- [45] Krutmann J, Schroeder P. Role of mitochondria in photoaging of human skin: the defective powerhouse model. *J Invest Dermatol Symp Proc* 2009; 14: 44-49.
- [46] Lin F H, Lin J Y, Gupta R D *et al.* Ferulic acid stabilizes a solution of vitamins C and E and doubles its photoprotection of skin. *J Invest Dermatol* 2005; 125: 826-832.
- [47] Kligman, L H. The hairless mouse model for photoaging. *Clin Dermatol* 1996; 14: 183-195.

- [48] Kligman L H, Mezick J A, Capetola R J, Thorne E G. Lifetime topical application of tretinoin to hairless mice. *Acta Derm Venereol* 1992; 72: 418-422.
- [49] Peres P S, Terra V A, Guarnier F A, Cecchini R, Cecchini A L. Photoaging and chronological aging profile: Understanding oxidation of the skin. *Journal Photochem Photobiol B Biol* 2011; 103: 93-97.
- [50] Schwartz E, Sapadin A N, Kligman L H. Ultraviolet B radiation increases steady-state mRNA levels for cytokines and integrins in hairless mouse skin: modulation by topical tretinoin. *Arch Dermatol Res* 1998; 290: 137-144.
- [51] Quan T, Qin Z, Robichaud P, Voorhees J J, Fisher G J. CCN1 contributes to skin connective tissue aging by inducing age-associated secretory phenotype in human skin dermal fibroblasts. *J Cell Commun Signaling* 2011; 5: 201-207.
- [52] Varani J, Warner R L, Gharaee-Kermani M *et al.* Vitamin A antagonizes decreased cell growth and elevated collagen-degrading matrix metalloproteinases and stimulates collagen accumulation in naturally aged human skin. *J Invest Dermatol* 2000; 114: 480-486.
- [53] Fisher G J, Kang S, Varani J *et al.* Mechanisms of photoaging and chronological skin aging. *Arch Dermatol* 2002; 138: 1462-1470.
- [54] Hernandez Cruz A , Garcia-Jimenez S, Zucatelli Mendonca R, Petricevich V L. Pro- and anti-inflammatory cytokines release in mice injected with *Crotalus durissus terrificus* venom. *Mediators Inflamm* 2008; 874962.
- [55] Nyati K K, Prasad K N, Rizwan A, Verma A, Paliwal V K. TH1 and TH2 response to *Campylobacter jejuni* antigen in Guillain-Barre syndrome. *Arch Neurol* 2011; 68: 445-452.
- [56] Kidd P. Th1/Th2 balance: the hypothesis, its limitations, and implications for health and disease. *Altern Med Rev* 2003; 8: 223-246.

- [57] Asadullah K, Sterry W, Stephanek K *et al.* IL-10 is a key cytokine in psoriasis. Proof of principle by IL-10 therapy: a new therapeutic approach. *J Clin Invest* 1998; 101: 783-794.
- [58] Kim Y K, Jung H G, Myint A M, Kim H, Park S H. Imbalance between pro-inflammatory and anti-inflammatory cytokines in bipolar disorder. *J Affect Disord* 2007; 104: 91-95.